IX International Conference on Computational Methods for Coupled Problems in Science and Engineering
COUPLED PROBLEMS 2021
E. Oñate, M. Papadrakakis and B. Schrefler (Eds)

NUMERICAL SIMULATION OF FLUID-STRUCTURE INTERACTION FOR THIN FLAT DELTA WING AT TRANSONIC SPEED BASED ON OPEN-SOURCE SOFTWARE

YUSUKE TAKAHASHI*

*Hokkaido University
Kita 13 Nishi 8, Kita-ku, Sapporo, Hokkaido 060-8628, Japan
e-mail: ytakahashi@eng.hokudai.ac.jp

Key words: Coupled Problems, Fluid-Structure Interaction, Transonic Flutter, Limit-Cycle Oscillation, Open-Source Software

Abstract. The flutter of a thin flat-delta wing at transonic speed was investigated by fluid-structure interaction (FSI) analysis, which is based on the open-source software. The analysis model was composed of fluid solver SU2, structure solver CalculiX, and coupler preCICE library. The FSI coupling of both solvers was performed in a partitioned approach. The software and libraries were built on a cloud computing system in Hokkaido University. It was found that self-induced oscillation of the delta wing is induced by the shock wave and elastic deformation in the transonic regime. The primary frequency of the oscillation was approximately 20 Hz for all speeds considered herein. However, the eigenfrequencies of the present condition of the delta wing, which are 9.62, 36.69, 51.22, 88.94, etc., did not correspond to the oscillation frequency. The phase delay of aerodynamic force for the deformation of the delta wing appeared in the oscillation. It was indicated that the oscillation is amplified by the aerodynamic force at the low deformation phase, and that is attenuated at a high deformation phase. In other words, in one cycle, the wing is in an unstable state by receiving the energy from fluid flow at the low deformation and is in a stable state by passing the energy to fluid flow at high deformation. When this energy transfer is equilibrated, the oscillation reaches the limit cycle. It was found that this behavior of the delta wing at the transonic speed is attributed to the shock wave and elastic deformation, i.e., coupling between flow and structure.

1 INTRODUCTION

Fluid-structure interaction (FSI) is a significant topic for mechanical engineering and aerospace engineering. Examples of FSI problems in high enthalpy flows which appear in rocket launching and atmospheric entry include aeroelastic problems in the fins or

body of rockets, coupling of aerodynamic forces and membrane aeroshells in inflatable reentry vehicles [1, 2], and behavior of parachute during descent. These are issues that require careful consideration in design and development because they can cause significant problems in some cases.

Estimations using wind tunnel facilities is important for FSI problems. However, it is difficult to reproduce actual conditions because the scale law can not always be applied. Numerical analysis removes this limitation and is expected to play a certain role in research and development. Single-physics problem such as flow and structure have been studied extensively, and the software for analysis has become quite sophisticated. On the other hand, however, there is still not much software available to deal with multiphysics problems such as FSI analysis. This is especially notable under limited conditions such as high enthalpy flows.

In recent years, many open-source software (OSS) have developed. OSS is becoming possible to solve various problems with a high degree of freedom. For example, SU2 [3], a compressible fluid analysis software, and CalculiX [4], a finite element analysis software, are ones of OSS. These are basically software for single-physics problems and have been used mainly for that purpose. Recently, an OSS coupling library called preCICE [5] has been developed, which enables to couple multiple software by simply preparing a small program called an adapter. An FSI analysis model that combines SU2 and CalculiX with preCICE are already available. This makes it possible to perform FSI under high enthalpy flows.

Transonic flutter [6] is one of the important FSI issues. This is caused by aeroelasticity, which is a combination of aerodynamic, elastic, and inertial forces. Once flutter occurs, destructive oscillation can occur to the aircraft and spacecraft. The flutter can be caused by the transonic dip, which tends to cause instability in the transonic region, and by the limit cycle oscillation, which has a constant amplitude of oscillation without destructive oscillation. Unsteady aerodynamic forces play a major role in flutter, and an appropriate structure analysis model is necessary to evaluate the elastic forces. The coupling between the aerodynamic and elastic problems plays an important role in the analysis, which requires large computational resources.

In recent years, it has become easier to use relatively-large computational resources, and FSI analysis software for high enthalpy flows has been developed. In this paper, the results of the FSI analysis of flutter in the transonic region using these software are reported.

2 FSI MODELING

The present FSI analysis model consists of SU2 fluid analysis software for unstructured grids as a flow solver, CalculiX finite element analysis software as a structure solver, and preCICE library as a coupler. The software with preCICE adapters [7] is available on Github.

2.1 Analysis Object

A thin flat delta wing with an isosceles triangle shape is placed in a freestream transonic flow with no angle of attack. As shown in Fig. 1, the delta wing has 40 mm sides and 1 mm thickness. The fixed points are the isosceles connecting the vertices "AC" shown in Fig. 1.

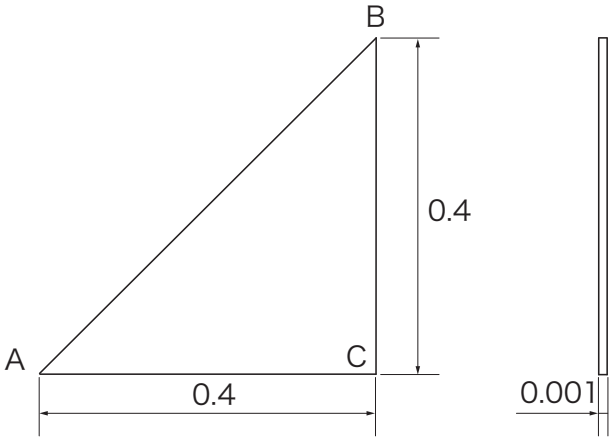

Figure 1: Sketch of delta wing. (All length dimensions are in millimeters.)

2.2 Flow Solver

The governing equations are the compressible Navier-Stokes equations and the equation of state for an ideal gas. The equations consist of the total density, momentum, and total energy conservation laws. The thermodynamic properties of the ideal gas are assumed to be the same as those of air at room temperature. The viscosity coefficient is evaluated using Sutherland's equation. The thermal conductivity is evaluated using the viscosity coefficient, the specific heat of constant pressure, and the Prandtl number of 0.72.

The governing equations are discretized in a finite volume manner. The control volume is defined as the node center. No turbulence model is assumed. The spatial gradients are calculated by the Green-Gauss method. The Jameson-Schmidt-Turkel (JST) scheme [8] is used for the advection term evaluation. The artificial viscosity coefficients in the JST scheme are set to 0.5 for the second order and 0.02 for the fourth order. The viscosity term is evaluated as the average value between neighboring cells for the spatial gradient of flow variables. Time integration is performed implicitly using the dual-time stepping. Local time stepping is used for the inner iteration, and global time stepping is used for the outer iteration to efficiently perform time integration. Since the outer iteration uses backward differencing with second-order accuracy, the accuracy in the time direction is also second-order if the inner iteration is sufficiently converged. The inversion of the coefficient matrix is necessary for the inner iteration. The GMRES method, which incorporates the LU-SGS method as preprocessing, is used here as the matrix solution method.

SU2-v6.0.0, which is a version installing preCICE adapter, is used as the flow solver, which supports unstructured grids data and has high shape reproducibility. The parallel computation is performed using the domain decomposition method and the message passing interface (MPI). Domain decomposition is performed by ParMETIS [9], which is a standard parallel method for flow simulations on large scale computers and can be used on various computers.

2.3 Structure Solver

The structural dynamics equations are described based on the principle of virtual work . Since the temperature change inside the object is not considered here, the momentum equilibrium of the displacement field is obtained. The equation is discretized by small elements and consists of the displacement in each element, the element stiffness matrix, the element load vector, and the element mass matrix. The element mass matrix is calculated by using the shape function used in the formulation of the element stiffness matrix.

By defining the displacement vector, the stiffness equation consisting of the stiffness matrix, the mass matrix, and the load vector can be obtained. The node displacements can be obtained by solving this equation under certain constraint conditions. In addition, the reaction force at the constraint point is obtained, and the strain and stress of each element are calculated.

Calculix v2.15, which is a version installing preCICE adapter, was used as the structure solver. A three-dimensional 10-node tetrahedral quadratic element was also used to discretize the object. In order to obtain the load vector, stiffness matrix, and mass matrix, numerical integration for each element is required. Here, Gauss–Legendre quadrature is used. The α-method [10] is used to solve the stiffness equation. This algorithm is second-order accurate and unconditionally stable when the parameter $\alpha \in [-1/3, 0]$, which is set $\alpha = -1/3$ here. In addition, the analysis is performed in geometrically nonlinear mode to handle large deformations. To do this, iterative calculations are required, which increases the amount of calculation. The material properties are assumed to be linear.

2.4 Coupling Method

The coupled method employed in preCICE is classified as a partitioned coupling, i.e., weakly coupling. Flow simulation and structure simulation are performed by the independent software mentioned above. Data for the coupled interface is passed between each other via the preCICE library. At this time, the continuity and equilibrium conditions between data are assumed to exist at the coupled interface.

The present coupled interface is the entire surface of the flat wing. The physical variables passed at the coupled interface are aerodynamic force on the flow solver and displacement on the structure solver. The computational grids at the coupled interface are necessarily not the same for both the flow and structure solvers. Even if the two

computational grids are different, data can be mapped and interpolated appropriately. Nearest-projection mapping is used here for the interpolation.

Data communication between the flow and structure solvers is performed using TCP/IP sockets.

To satisfy the continuity and equilibrium conditions, an implicit coupling scheme is adopted. That iterates through the fluid-structure partitioned system in a single time step. In the case of an implicit coupling scheme, the coupling can be performed more efficiently by introducing an appropriate convergence acceleration scheme or stabilization scheme in the iterations. Here, the interface quasi-Newton method [11] is adopted.

PreCICE v1.61, which implements these methods, is adopted.

2.5 Computational Conditions

Figure 2 shows the computational grids for the flow simulation. A flat delta wing is set to be placed in a freestream flow. The reservoir pressure, temperature, and Mach number are given as freestream conditions. The freestream parameters are determined from the equation of the isentropic process. In this study, Mach numbers of 0.9 and 1.1 are used for the cases of reservoir pressures of 1000, 5000, 8000, and 10000 Pa, and reservoir temperatures of 300 K are used. When the characteristic length is 0.4 m, the Reynolds number is of the order of 10^5. The angle of attack is set to zero. The wing surface is assumed to be fixed at 300 K, no slip, and no pressure gradient in the normal direction. All computational grids consist of tetrahedral grids. The number of computational cells is 2,111,38 and the number of computational nodes is 363,255.

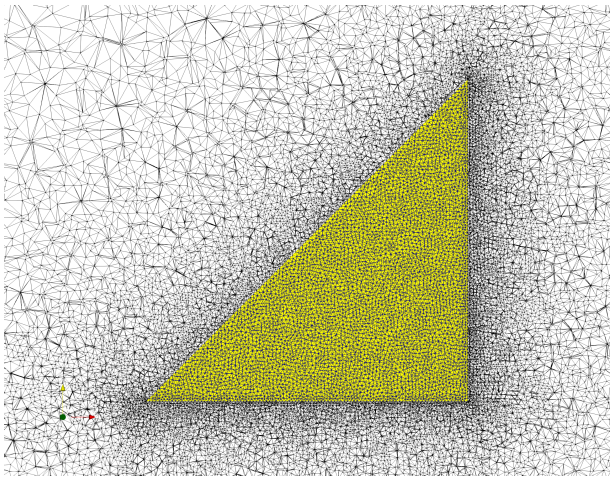

Figure 2: Computational grids for flow solver SU2.

The computational mesh used for the structure simulation is shown in Fig. 3. This mesh also consists of tetrahedral shapes, but quadratic elements are considered to improve the accuracy. The number of nodes is 154,932. One side of the delta wing is set as a

fixed boundary. All the others are free boundaries and coupled interfaces. The wing is assumed to be composed of a single material. The mechanical properties of the material are assumed to be similar to those of an aluminum alloy, with a Young's modulus of 74 GPa, a Poisson's ratio of 0.355, and a density of 2800 kg/m^3.

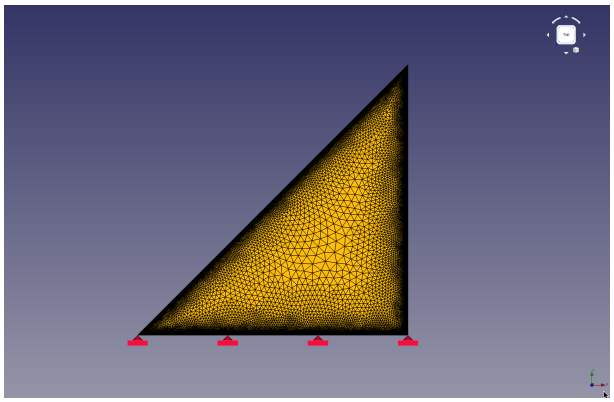

Figure 3: Computational mesh for structure solver CalculiX.

The intercloud system of the Information Initiative Center of Hokkaido University is used as a computation server. Users can freely change the system including the operating system. In this case, the solvers and dependent libraries were installed on Ubuntu 16.04 LTS. For the FSI analysis, distributed memory parallel processor with domain decomposition and MPI for the flow solver, and shared memory parallel processor with OpenMP for the structural solver are used. The number of parallel for each is 16 for flow simulation and 4 for structure simulation.

3 RESULTS AND DISCUSSION

The time histories of the displacements were investigated by using probe technique into one of the three vertices of the delta wing that do not contain a fixed boundary, i.e., vertex "B" in Fig. 1. The displacement histories in the z-direction for freestream Mach numbers of 0.9 and 1.1 is shown in Fig. 4 for each dynamic pressure condition. At a high dynamic pressure of 8000 Pa, self-induced oscillations are observed. On the other hand, at low dynamic pressures of 1000 and 5000 Pa, small oscillations occur, but large self-induced oscillations are not caused. At Mach number 0.9, the self-induced oscillation settles down to a constant amplitude and the limit cycle is confirmed, whereas at Mach number of 1.1, the displacement still tends to increase in this period. The self-induced oscillation with some large amplitude indicates the existence of a certain Mach number region and dynamic pressure region.

Fast Fourier transform (FFT) was performed on the displacement histories from 0 to 0.5 s. The Hamming window function was used. Figure 5 shows the condition of Mach number 1.1 and dynamic pressure 10000 Pa. In this condition, a peak at 64 Hz can be

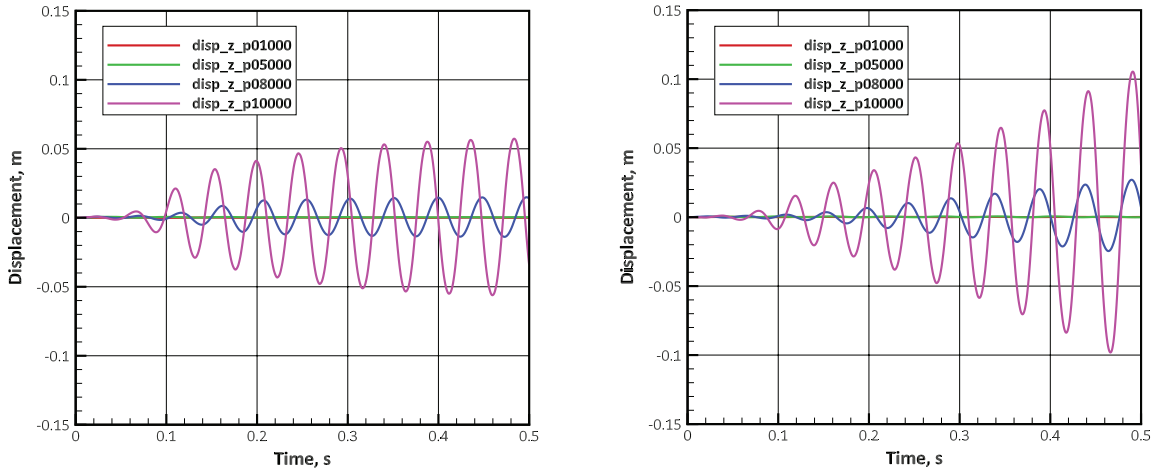

(a) freestream Mach number of 0.9.

(b) freestream Mach number of 1.1.

Figure 4: History of displacement in z-direction of wing tip.

observed in addition to the 22 Hz peak. However, it can be inferred from the displacement history that the 64 Hz peak is not so dominant. The eigenfrequencies up to mode 8 of the single-end fixed delta wing used in this study are shown in Table 1. As mentioned above, the self-induced oscillation frequency of FSI in the transonic region of 20 Hz does not correspond to the eigenfrequency. Therefore, the self-induced oscillation is not caused by the coincidence of the characteristic frequency of the fluid motion and the eigenfrequency of the object, but is considered to be caused by another mechanism.

Table 1: Eigenfrequency of the present delta wing.

Mode	Frequency, Hz
1	9.62
2	36.69
3	51.22
4	88.94
5	122.40
6	158.89
7	181.68
8	217.62

The time series distributions of Mach number near the delta wing and pressure coefficient at the delta wing surface for the case of freestream Mach number of 1.1 and reservoir

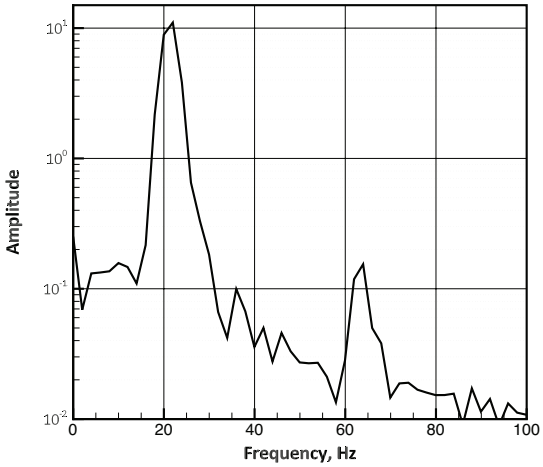

Figure 5: FFT result for displacements history for the case of Mach number of 1.1 and reservoir pressure of 10000 Pa.

pressure of 10000 Pa are shown in Fig. 6. The Mach number distribution is for the y=0.15 m section of the computational domain. In this figure, the freestream is flowing from the right side to the left side. These are for times t = 0.429, 0.441, 0.454, and 0.466 s. Figures 6(a), 6(b), 6(c), and 6(d) show the times of almost minimum displacement with positive displacement velocity in the z direction, maximum displacement at this time, almost minimum displacement with negative displacement velocity in the z direction, and maximum displacement at this time, respectively (See also Fig. 4(b)). Shock waves are formed in front of the delta wing, and a boundary layer appears near the surface. A separated shear layer deriving from the boundary layer extends far in the wake. In Fig. 6(b), t = 0.441 s is the time when the displacement in the z-direction reaches its maximum in the positive direction. Shock waves are generated on the upper surface of the wing in the positive z-direction, while no shock waves are generated on the lower surface. At t=0.466 s in Fig. 6(d), the time when the displacement in the z-direction reaches its maximum in the negative direction. Shock waves are generated on the lower surface of the wing, while they do not appear on the upper surface of the wing.

The background of the increase in the amplitude of the self-induced oscillation is considered to be the aerodynamic force that drives it. Figure 7 shows the time histories of the z-direction displacement of the wing tip and the lift force acting on the wing. For comparison, the axes of the lift coefficient are reversed. The freestream conditions are Mach number 1.1 and reservoir pressure 10000 Pa. As the relationship between displacement and lift, a profile like van der Pol oscillator appears. Such a relationship is also confirmed by the pitch instability in the transonic region of the Hayabusa sample return capsule [12].

In the case of a thin wing in the transonic region of this study, when the initial dis-

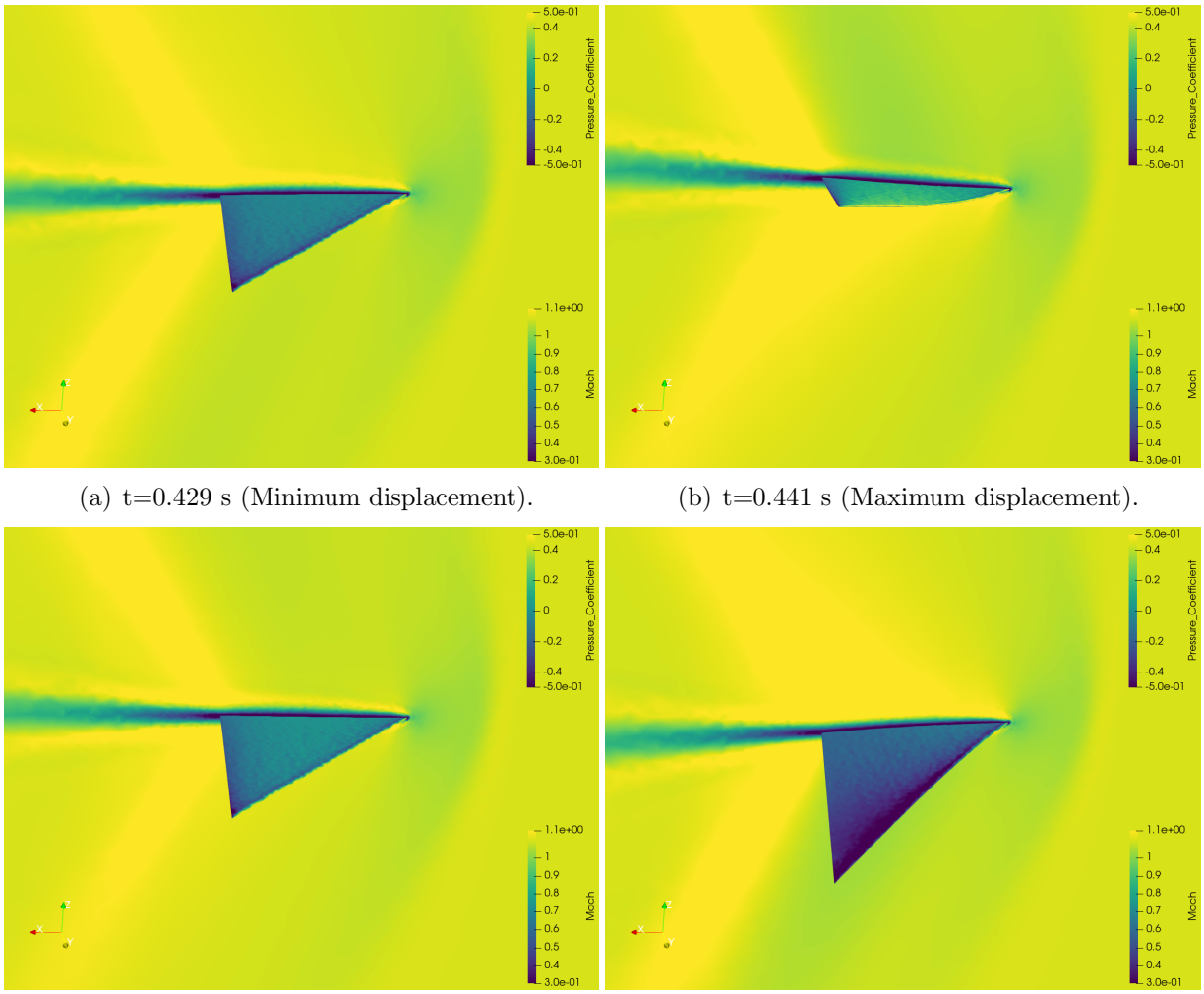

(a) t=0.429 s (Minimum displacement).

(b) t=0.441 s (Maximum displacement).

(c) t=0.454 s (Minimum displacement).

(d) t=0.466 s (Maximum displacement).

Figure 6: Distributions of Mach number near wing and pressure coefficient on wing surface for the case of Mach number of 1.1 and reservoir pressure of 10000 Pa.

turbance causes oscillation, shock waves are generated asymmetrically on the upper and lower surfaces of the wing. The high-pressure region behind the shock wave on one side of the wing tries to suppress the oscillation, while its response is accompanied by a slight delay, which acts as a phase delay of the external force against the oscillation. It is indicated that this is switched between negative and positive damping depending on the amount of displacement, resulting in self-induced oscillation. Therefore, the local elastic deformation produced by the shock wave plays a major role in the instability of the thin wing in the transonic region. In other words, the tight coupling between aerodynamics and elasticity has a large influence on the self-induced oscillation.

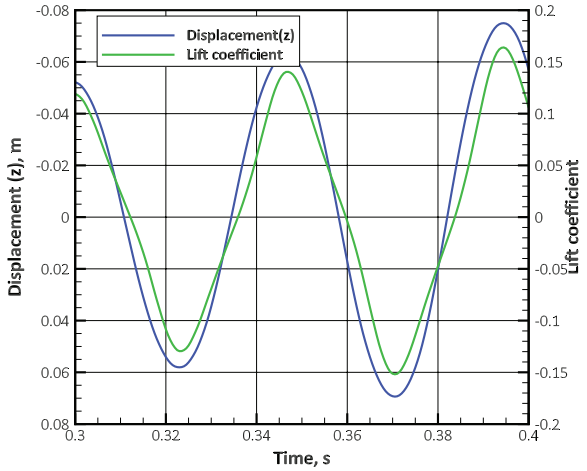

Figure 7: Histories of displacement of wing tip and lift coefficient for the case of Mach number of 1.1 and reservoir pressure of 10000 Pa.

4 CONCLUSIONS

An open-source software-based fluid-structure interaction (FSI) analysis model had been developed for the flutter of a flat delta wing in the transonic regime, and its behavior had been clarified. The FSI model was based on unsteady viscous flow analysis using a compressible flow solver and a geometrically nonlinear structural analysis using a finite element-based solver, and the two were coupled by a coupling library.

The FSI analysis showed that the self-induced oscillation is caused by the condition of freestream Mach number and reservoir pressure. In particular, large self-induced oscillations occurred in the range of freestream Mach numbers 0.9 and 1.1. The oscillation frequency was about 20 Hz regardless of the freestream conditions. This suggested that the characteristic oscillation phenomenon of the flow does not cause unstable oscillation on the structure in the form of resonance, since there is no corresponding eigenfrequency of the present delta wing. In the case of significant self-induced oscillation, the shock wave on the wing surface formed a local high-pressure region. This induced a local elastic deformation of the wing, resulting in oscillation. The aerodynamic force acting on the wing against displacement was accompanied by a phase delay. The aerodynamic forces acted to promote the instability of the oscillation at small displacements, and acted as a damping mechanism at large displacements. These results suggested that, for an oscillation with a certain amplitude, the energy transfer between destabilization and stabilization reaches equilibrium within a cycle, and the oscillation eventually falls into a limit cycle.

ACKOWLEDGMENTS

This work was supported by JSPS KAKENHI Grant Number 20H02360. This work was supported by "Joint Usage/Research Center for Interdisciplinary Large-scale Information Infrastructures" and "High Performance Computing Infrastructure" in Japan (jh200035).

REFERENCES

[1] Y. Takahashi and K. Yamada. "Aerodynamic heating of inflatable aeroshell in orbital reentry". *Acta Astronautica*, 152:437 – 448, 2018.

[2] Y. Takahashi, T. Koike, N. Oshima, and K. Yamada. "Aerothermodynamic analysis for deformed membrane of inflatable aeroshell in orbital reentry mission". *Aerospace Science and Technology*, 92:858–868, 2019.

[3] T.D. Economon, F. Palacios, S.R. Copeland, T.W. Lukaczyk, and J.J. Alonso. "SU2: An open-source suite for multiphysics simulation and design". *Aiaa Journal*, 54(3):828–846, 2016.

[4] G. Dhondt and K. Wittig. "Calculix a free software three-dimensional structural finite element program". `www.calculix.de`.

[5] H.J. Bungartz, F. Lindner, B. Gatzhammer, M. Mehl, K. Scheufele, A. Shukaev, and B. Uekermann. "preCICE–a fully parallel library for multi-physics surface coupling". *Computers & Fluids*, 141:250–258, 2016.

[6] O.O. Bendiksen. "Review of unsteady transonic aerodynamics: Theory and applications". *Progress in Aerospace Sciences*, 47(2):135–167, 2011.

[7] "preCICE". `https://github.com/precice`.

[8] A. Jameson. "Origins and further development of the Jameson–Schmidt–Turkel scheme". *AIAA Journal*, 55(5):1487–1510, 2017.

[9] G. Karypis, K. Schloegel, and V. Kumar. "Parmetis: Parallel graph partitioning and sparse matrix ordering library". 1997.

[10] I. Miranda, R.M. Ferencz, and T.J.R. Hughes. "An improved implicit-explicit time integration method for structural dynamics". *Earthquake Engineering & Structural Dynamics*, 18(5):643–653, 1989.

[11] J. Degroote, P. Bruggeman, R. Haelterman, and J. Vierendeels. "Stability of a coupling technique for partitioned solvers in FSI applications". *Computers & Structures*, 86(23-24):2224–2234, 2008.

[12] K. Hiraki. “Transonic Dynamic Instability of disk-shaped Capsule”. *The Institute of Space and Astronautical Science report. SP Aerodynamics, Thermophysics, Thermal Protection, Flight System Analysis and Design of Asteroid Sample Return Capsule*, 17:265, 2003.